

## Observation of Sawtooth Oscillations in the COMPASS Tokamak

M. Imříšek,<sup>1,2</sup> J. Havlíček,<sup>1,2</sup> V. Weinzettl,<sup>2</sup> J. Mlynář<sup>2</sup>

<sup>1</sup> Charles University in Prague, Faculty of Mathematics and Physics, Prague, Czech Republic.

<sup>2</sup> Institute of Plasma Physics AS CR, v.v.i., Prague, Czech Republic.

**Abstract.** The sawtooth instability in tokamak plasmas results in periodic relaxations of the core plasma density and temperature. The physics of sawtooth is still not fully understood. It is predicted that fusion-born alpha particles will lead to long sawteeth. However, longer sawteeth can seed other instabilities which cause further degradation of plasma confinement. This paper provides brief introduction into sawtooth physics and observations of sawtooth instability in COMPASS. Furthermore, evidence of triggering transition to high confinement regime by sawtooth crash is presented.

### Introduction

Tokamaks are supposed to be operated close to their limits to provide the best possible energy gain. Besides material limitations, there is a variety of plasma instabilities causing degradation of plasma confinement or even an abrupt termination of the plasma. The sawtooth oscillation is one of the fundamental instabilities in tokamak. It is associated with repetitive slow increases and fast drops in both the core temperature and density which can be consequently seen as a sawtooth pattern on several diagnostics.

A typical sawtooth cycle consists of three phases: stable ramp phase during which both the core plasma density and temperature increase, precursor phase with growth of magnetic perturbation and fast collapse phase when both the central temperature and density drop rapidly.

Fast collapse phase is accompanied by the heating of the edge plasma. Temperature profile is flattened during the collapse. Radius, where temperature does not change during collapse, is called the inversion radius. Although this instability affects significant volume of the plasma, it rarely leads to a termination of a discharge.

The sawtooth instability is one of important topics in fusion physics for several reasons. Fusion-born  $\alpha$  particles are predicted to lead to longer sawtooth period. However, longer sawteeth were shown to trigger other instabilities below their threshold which lead to further degradation of plasma confinement. It is possible to avoid sawteeth in some operational scenarios, However, sawteeth instabilities can also be beneficial, because they can help to remove helium ash and impurities from plasma core. Therefore, short controlled sawteeth are included in some baseline scenarios for ITER. Period of these sawteeth has to be well controlled, because it should be short in order to prevent seeding other instabilities but longer than the slowing down time of  $\alpha$  particles. It is also observed that sawtooth instability can trigger transition to a state with better plasma confinement (H-mode). This transition is still not completely understood. Furthermore, recent observations of sawtooth oscillations in solar flare radio emission suggest that this instability can be universal for current carrying toroidal plasmas [1]. Therefore, understanding the sawtooth instability is beneficial for controlling fusion devices as well as for solar physics.

In this article, a brief introduction into physics of sawtooth instability is presented in the next section followed by observation of sawteeth in the COMPASS tokamak. Comparison with magnetic measurements and evidence of triggering transition from lower confinement to high confinement (L-H transition) by sawtooth collapse is also included.

### Physical background of sawtooth instability

The sawtooth crash is probably initiated by the internal kink mode [2]. Kink instability can develop in plasma column carrying a current. Poloidal magnetic field induced by toroidal plasma current enhances any deformation of plasma column, causing the “kinking” effect (see Figure 1a). Kink mode can be stabilized by magnetic field along plasma column (it takes energy to compress magnetic field lines). In tokamaks, external kink mode can lead to sudden termination of discharge (disruption). Internal kink mode causing the sawtooth crash does not move with plasma boundary and can take place when safety factor  $q$  goes below one. Safety factor represents average inverse pitch angle of magnetic field lines:

$$q = \frac{1}{2\pi} \oint \frac{r B_\phi}{R B_\theta} d\theta \quad (1)$$

where  $r$  is local minor radius and  $R$  major radius of plasma torus,  $B_\phi$  toroidal field and  $B_\theta$  poloidal field. When gradient of current density is too high, strong poloidal magnetic field generated by this plasma current can displace the central region of the plasma, which results in crowding of magnetic field lines on one side. According

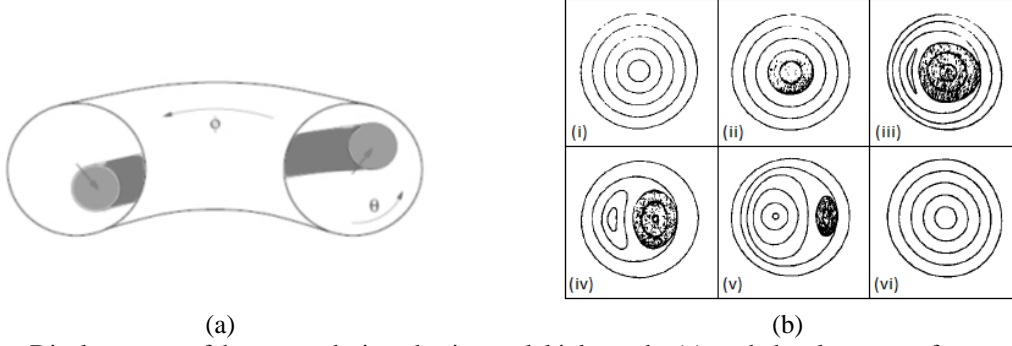


**Figure 1.** Displacement of hot core during the internal kink mode (a) and development of magnetic field structure in specific poloidal cross section (b) during the sawtooth instability according to Kadomtsev's model [1].

to the Kadomtsev model [2], magnetic X-point is formed on this side and magnetic island starts to grow. Hot core partially surrounded by this cooler island is then expelled to the edge and new cylindrically symmetric magnetic field structure is established. The development of magnetic field structure is depicted in Figure 1b.

The collapse time is in Kadomtsev model given by reconnection time as geometric mean of the resistive diffusion time  $\tau_R$  and the Alfvénic time  $\tau_A$ :

$$\tau_c \sim \sqrt{\tau_R \tau_A} = \sqrt{\left(\frac{\mu_0 r_1^2}{\eta}\right) \left(\frac{r_1 \sqrt{\mu_0 \rho}}{B_\theta (1-q)}\right)} \quad (2)$$

where  $r_1$  is inversion radius (it is radius where  $q = 1$ ),  $\rho$  plasma density,  $\eta$  plasma resistivity. However, observed collapse times are much shorter than times predicted by Kadomtsev model  $\tau_c r_1^{3/2}$  [2]. Furthermore,  $q$ -profile measurements indicate that  $q$  remains below one even after the collapse, which is in contradiction with Kadomtsev model in which island grows until it fills the whole volume inside the magnetic surface of  $q = 1$ .

Alternative sawtooth crash trigger models, including quasi-interchange model [2], ballooning mode model and others [3] were proposed. However, these models are not consistent with recent measurements of electron temperature by electron cyclotron emission imaging system with high spatial and temporal resolution on the TEXTOR tokamak [4], where sawtooth crash was observed to occur in non-chaotic way and hot plasma surged through X-point of the instability, which was localized also in the region of good curvature (X-point on inner side of torus is in contradiction with ballooning theory). Currently, the mostly accepted sawtooth crash trigger model is the partial reconnection model, which is not in conflict with electron temperature measurements on TEXTOR and  $q < 1$  after the sawtooth collapse. The partial reconnection model is similar to Kadomtsev model but magnetic island grows only until it reaches its critical width. Consequently, two current sheets are formed diffusing rapidly during the next sawtooth ramp [3]. However, the dynamics of sawtooth instability is influenced by many other phenomena including the effect of sheared flows, collisionless kinetic effects related to high energy particles and thermal particles, and non-ideal effects localized around  $q = 1$ . Porcelli proposed a heuristic model [5] predicting that sawtooth is triggered when one of three criteria is met. For example, most relevant criterion for plasmas with energetic ions (auxiliary heated plasmas) is:

$$\pi \frac{\delta \hat{W}}{s_1} < c_\rho \frac{\rho}{r_1} \quad (3)$$

where  $\rho$  is ion Larmor radius,  $r_1$  inversion radius,  $c_\rho$  normalization coefficient,  $s_1$  magnetic shear at  $q = 1$  surface:

$$s_1 = \left. \frac{r}{q} \frac{dq}{dr} \right|_{q=1} \quad (4)$$

and  $\delta \hat{W}$  is normalized change in potential energy of internal kink mode:

$$\delta \hat{W} = \frac{4}{s_1 \xi_0^2 \varepsilon_1^2 R B^2} \delta W = \frac{4}{s_1 \xi_0^2 \varepsilon_1^2 R B^2} (\delta W_{MHD} + \delta W_{KO} + \delta W_h) \quad (5)$$

where  $\delta W_{MHD}$  is change in ideal magnetohydrodynamic energy [6],  $\delta W_{KO}$  contribution of the collisionless thermal ions [2,7] and  $\delta W_h$  change in the energy due to the fast ions [3]. In the normalization term, there is  $\xi_0$  as radial displacement of magnetic axis,  $\varepsilon_1 = r_1/R$  and  $B$  magnetic field. As it can be seen from the condition (3),

sawtooth crash is triggered when the magnetic shear at  $q = 1$  surface is sufficiently large or when the change in potential energy of internal kink mode  $\delta\widehat{W}$  is sufficiently small (it is based on energy principle). Numerical simulations based on Porcelli's model are in agreement with observed sawtooth period [8]. Magnetic shear can be changed through localized electron cyclotron current drive (ECCD) and potential energy through neutral beam injection (NBI) or ion cyclotron resonance heating (ICRH), because both NBI and ICRH affect distribution of fast particles. Sawtooth instability was successfully controlled on many tokamaks in this way [3].

### Sawtooth oscillations in COMPASS

Sawtooth oscillations in plasma core density and temperature can be clearly observed using soft x-ray (SXR) detectors. Soft X-rays are in tokamaks mainly generated as bremsstrahlung, which is given by electron-ion collisions (radiation fields produced by the two particles in like-particle collision exactly cancel in the nonrelativistic limit), and thus, SXR power depends on both density and temperature:

$$P_{brem} \sim Z_{eff} n_e^2 \sqrt{T_e} \quad (6)$$

where  $T_e$  is electron temperature,  $n_e$  electron density,  $Z_{eff} = \sum_i n_i Z_i / n_e$  effective charge,  $n_i$  ion density and  $Z_i$  ion charge. Sawtooth oscillations on the COMPASS tokamak (major radius  $R = 0.56$  m, minor radius  $a = 0.18$  m,  $B_T = 1.15$  T, ITER-like plasma geometry) [9] presented in this article were measured by the pinhole camera with array of 35 photodiodes (same type LD 35-5T is used also on JET [10] and ASDEX-U [11]) shielded by  $10\mu\text{m}$  Be foil to block low energy photons below 1eV [12]. Upper limit of spectral sensitivity is given by thickness of diode active layer  $d_{active} = 200\mu\text{m}$ . The radiation is also slightly absorbed by diode passivation layer with thickness  $d_{Si_3N_4} = 0.55\mu\text{m}$  and diode dead layer with thickness  $d_{dead} = 0.6\mu\text{m}$ . Resulting spectral sensitivity is (see Figure 2a):

$$f(E) = \exp(-\mu_{Be}d_{Be} - \mu_{Si}d_{dead} - \mu_{Si_3N_4}d_{Si_3N_4}) \cdot (1 - \exp(-\mu_{Si}d_{active})) \quad (7)$$

where  $\mu_{Be}$ ,  $\mu_{Si}$ ,  $\mu_{Si_3N_4}$  are absorption coefficients. Temporal resolution of SXR detectors is up to  $1\mu\text{s}$  and spatial (given by field of view of detectors through the small pinhole) about 1–2 cm in the plasma centre. Lines of sight of SXR detectors cover almost the whole poloidal cross section of the vacuum vessel, as it can be seen in Figure 2b.

Figure 3 illustrates an example of sawtooth oscillations in COMPASS on three chosen SXR signals coming from plasma core, plasma edge and from region of inversion radius. The signal from plasma core has a clear sawtooth shape, while the signal from plasma edge exhibits reverse sawteeth as a result of heat expelled from the plasma core. Finally, the signal from the region of inversion radius corresponds to transition between regular and reverse sawteeth. In the shot 4415, both neutral beam injectors were switched on with total power about 630 kW (power transferred to plasma is, however, lower) causing sawteeth with a longer period — about 6 ms. Sawtooth observed without NBI typically lasts less than 3 ms.

### Time evolution of sawtooth instability

Figure 4 displays a detail of one sawtooth cycle together with several connected plasma parameters — poloidal magnetic field, intensity of H $\alpha$  radiation and hard X-rays (HXR). During the precursor phase, there are oscillations of poloidal magnetic field and SXR signal (with the same frequency  $\approx 16.6$  kHz) which represent

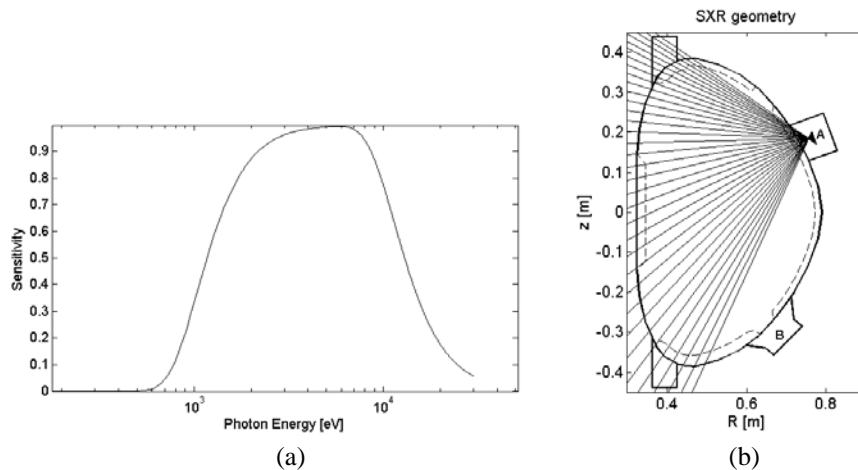


**Figure 2.** Spectral sensitivity (a) and geometry (b) of used SXR detectors.

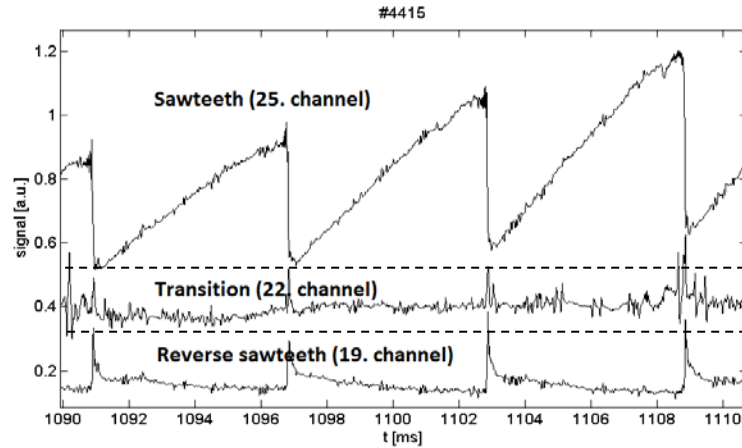


**Figure 3.** Representative SXR signals during the sawtooth instability. There is a clear sawtooth pattern on the intensity of SXR from plasma core, reverse sawtooth pattern on SXR from plasma edge and a pattern corresponding to transition between regular and reverse sawtooth on SXR signal.

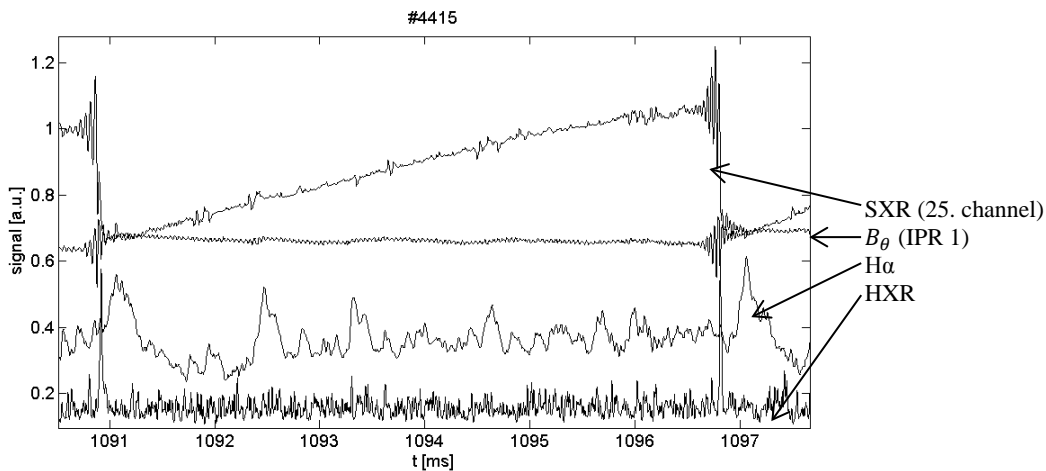


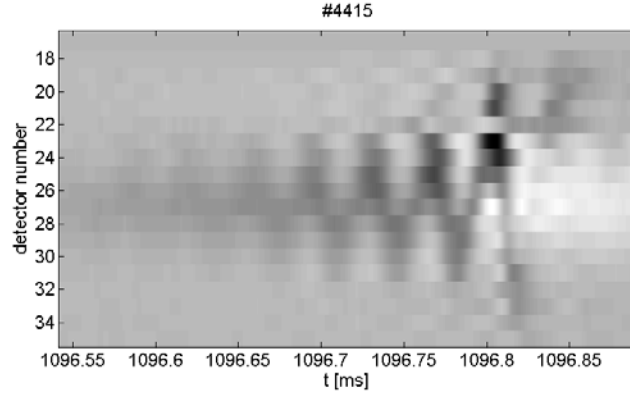
**Figure 4.** Detail of one sawtooth cycle showing SXR from plasma core, signal corresponding to poloidal magnetic field (internal partial Rogowski coil 1) with oscillations during the precursor phase, HXR intensity with peak during the sawtooth collapse and the near-central chord of H $\alpha$  intensity.

internal kink mode development in rotating plasma. Sawtooth collapse is in this case accompanied by a peak on HXR signal which is probably caused by collisions of the lost fraction of fast electrons with the vessel. These fast electrons could be generated in the beginning of discharge (runaway electrons) and are expelled from the confined plasma during the crash.

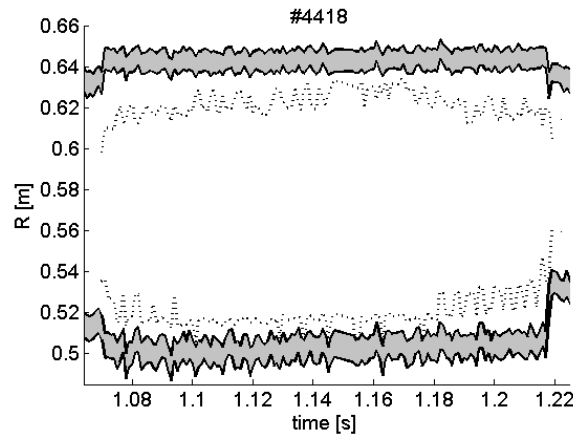
The development of internal kink mode during the precursor phase can be clearly seen in Figure 5. Displacement of the hot core during the internal kink mode (as shown in Figure 1a) and plasma rotation results in oscillations of SXR signals. Maximal intensity of these oscillations has a character of sine wave in radiation profile observed by SXR detectors due to the apparent poloidal rotation of hot core. Amplitude of this sine wave increases as the hot core shifts to the plasma edge until sawtooth crash. Time of the observed precursor phase was about 300 $\mu$ s.

### Comparison with magnetic measurements

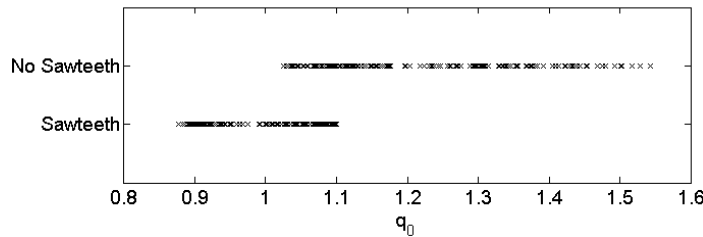
Figure 6 compares inversion radii calculated from magnetic measurements via EFIT [10] code (equilibrium fitting) as a magnetic surface, where  $q = 1$ , with inversion radii seen by SXR detectors as the closest positions to the plasma center, where reverse sawteeth are observed. If the theory is correct, the difference between inversion radii calculated from magnetic measurements and from SXR radiation could be caused by overestimation of  $q$  values near inversion radii by EFIT by 5 % to 10 % (Figure 7 also suggests imprecision of  $q$  in plasma centre about 10 %). This slight overestimation could be due to the fact that plasma current distribution assumed by EFIT may differ from real plasma current distribution. In some cases, it can be also difficult to distinguish reverse sawteeth from transition phase which can affect the precision of inversion radii calculated from SXR measurements.



**Figure 5.** SXR signals without trend during the precursor phase. Oscillations indicate the displacement of hot core in rotating plasma. Black color corresponds to maximum, white color corresponds to minimum.



**Figure 6.** Position of  $q = 1$  calculated from magnetic measurements (dotted line) and from SXR radiation (uncertainty given by the spatial resolution of SXR detectors is represented by grey area).



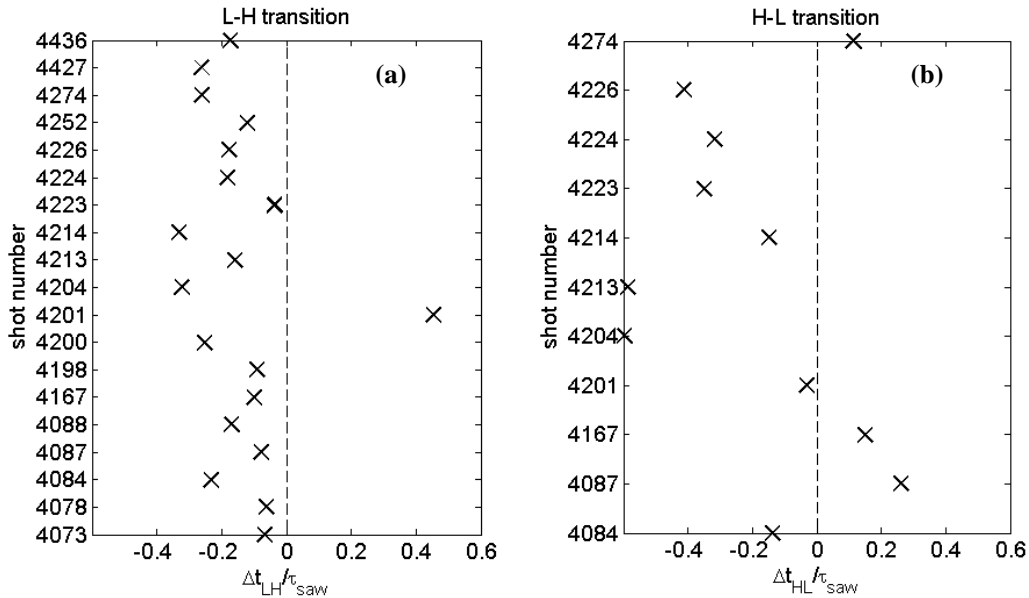
**Figure 7.** Safety factor  $q$  in plasma centre ( $q_0$ ) with and without sawtooth instability.

Figure 7 shows safety factor  $q$  in plasma centre ( $q_0$ ) with and without sawtooth activity. Safety factor  $q_0$  ranged from 0.88 to 1.1 in the presence of sawtooth instability. If the theory is correct, imprecision of  $q_0$  reconstructed by EFIT is about 10%.

### L-H and H-L transition

Physical mechanism leading to L-H transition is still not fully understood. When plasma is heated sufficiently (threshold heating power is exceeded), it may spontaneously reorganize to high confinement state (H-mode). In the H-mode, edge transport barrier is established due to the suppression of turbulences at the plasma edge. This process is probably a consequence of sheared flows (tearing the turbulences) and an associated edge radial electric field [2].

One of mechanisms which can trigger the L-H transition is the sawtooth crash, as can be seen in Figure 8a. This mechanism is not clear yet, but it is supposed that hot plasma expelled from the central region to the edge can supply enough free energy to the formation of the edge transport barrier. Conversely, H-L transition should not be triggered by the sawtooth crash, which corresponds to their mutual random phasing (see Figure 8b).



**Figure 8.** Time delays between sawtooth crash and L-H transition (a) and H-L transition (b) normalized to sawtooth period ( $\tau_{saw}$ ). Negative values correspond to sawtooth crash before L-H (H-L) transition.

## Conclusion

Sawtooth instability is a significant phenomenon influencing many processes in plasma of the COMPASS tokamak. The development of internal kink mode during the precursor phase was clearly observed via oscillations of the SXR signals. Peak on the HXR signal during the sawtooth crash is probably caused by collisions of released runaway electrons with the vessel. Sawtooth instability was also used to cross-check the reconstruction of  $q$ -profile by the EFIT code. Reconstructed  $q$ -profiles are in agreement with observed sawtooth instability and estimated precision of reconstructed  $q$  is about 10 %. It was observed that L-H transition on COMPASS can be triggered by sawtooth crash.

**Acknowledgments.** I would like to thank all authors for their effort and collaborative spirit. This work was partly supported by MSMT Project # LM2011021.

## References

- [1] A. Klassen, 2001, *Astron. Astrophys.* 370, L41.
- [2] J. Wesson, 2004, *Tokamaks*, 3rd edition, Clarendon Press, Oxford.
- [3] I. T. Chapman et al., 2011, *Plasma Phys. Control. Fusion* 53 013001.
- [4] H. K. Park et al., 2006 *Phys. Rev. Lett.* 96 195004.
- [5] F Porcelli et al 1996, *Plasma Phys. Control. Fusion* 38 2163.
- [6] F. L. Waelbroeck 1996, *Phys. Plasmas* 3 1047.
- [7] M. L. Mayoral et al., 2004, *Phys. Plasmas* 11 2607.
- [8] I. T. Chapman et al., 2007, *Plasma Phys. Control. Fusion* 49 B385.
- [9] R. Panek et al., 2006, *Czechoslovak Journal of Physics* 56 (2006) B125–137.
- [10] B. Alper, et al., January 1997, *Rev. Sci. Instrum.*, Vol. 68, No. 1, 778–781.
- [11] V. Igochine, A. Gude, and M. Maraschek, 2010, IPP Report No. 1/338.
- [12] V. Weinzettl, et al., 2010, *Nuclear Instruments and Methods in Physics Research A* 623 806–808.
- [13] L. C. Appel, et al., 2006, 33rd EPS Conference on Plasma Physics, vol. 30I, p. 2.184.